Annals of Biomedical Engineering (© 2022)
https://doi.org/10.1007/s10439-022-03029-5

BMES BIOMEDICAL ENGINEERING SOCIETY

Original Article

Treatment Planning for Atrial Fibrillation Using Patient-Specific Models Showing the Importance of Fibrillatory-Areas

Roya Kamali,[1,2,3,6] Karli Gillete,[5] Jess Tate,[4] Devaki Abhijit Abhyankar,[1] Derek J. Dosdall,[1,2,3] Gernot Plank,[5] T. Jared Bunch,[2] Rob S. Macleod,[1,3] and Ravi Ranjan[1,2,3]

[1]Department of Biomedical Engineering, University of Utah, Salt Lake City, UT, USA; [2]Division of Cardiovascular Medicine, Department of Internal Medicine, University of Utah, Salt Lake City, UT, USA; [3]Nora Eccles Harrison Cardiovascular Research and Training Institute, University of Utah, Salt Lake City, UT, USA; [4]Scientific Computing and Imaging Institute, University of Utah, Salt Lake City, UT, USA; [5]Institute of Biophysics, Medical University of Graz, Graz, Austria; and [6]Department of Biomedical Engineering, Georgia Institute of Technology, Atlanta, GA, USA

(*Received 19 January 2022; accepted 18 July 2022*)

Associate Editor Stefan M. Duma oversaw the review of this article.

Abstract—Computational models have made it possible to study the effect of fibrosis and scar on atrial fibrillation (AF) and plan future personalized treatments. Here, we study the effect of area available for fibrillatory waves to sustain AF. Then we use it to plan for AF ablation to improve procedural outcomes. CARPentry was used to create patient-specific models to determine the association between the size of residual contiguous areas available for AF wavefronts to propagate and sustain AF [fibrillatory area (FA)] after ablation with procedural outcomes. The FA was quantified in a novel manner accounting for gaps in ablation lines. We selected 30 persistent AF patients with known ablation outcomes. We divided the atrial surface into five areas based on ablation scar pattern and anatomical landmarks and calculated the FAs. We validated the models based on clinical outcomes and suggested future ablation lines that minimize the FAs and terminate rotor activities in simulations. We also simulated the effects of three common antiarrhythmic drugs. In the patient-specific models, the predicted arrhythmias matched the clinical outcomes in 25 of 30 patients (accuracy 83.33%). The average largest FA (FA_{max}) in the recurrence group was 8517 ± 1444 vs. 6772 ± 1531 mm^2 in the no recurrence group ($p < 0.004$). The final FAs after adding the suggested ablation lines in the AF recurrence group reduced the average FA_{max} from 8517 ± 1444 to 6168 ± 1358 mm^2 ($p < 0.001$) and stopped the sustained rotor activity. Simulations also correctly anticipated the effect of antiarrhythmic drugs in 5 out of 6 patients who used drug therapy post unsuccessful ablation (accuracy 83.33%). Sizes of FAs available for AF wavefronts to propagate are important determinants for ablation outcomes. FA size in combination with computational simulations can be used to direct ablation in persistent AF to minimize the critical mass required to sustain recurrent AF.

Keywords—Computational atrial fibrillation model, Mechanisms of atrial fibrillation, Ablation, Magnetic resonance imaging, Atrial rotor activities.

ABBREVIATIONS

AF	Atrial fibrillation
LGE	Late gadolinium enhancement
MRI	Magnetic resonance imaging
FA	Fibrillatory area
RF	Radiofrequency

INTRODUCTION

Atrial fibrillation (AF) is the most common sustained cardiac arrhythmia and a major contributor to morbidity and mortality.[1] Radiofrequency (RF) ablation is a common treatment option for drug-resistant AF. The superiority of RF catheter ablation to antiarrhythmic drug therapy has been shown in many clinical trials reporting arrhythmia-free survival of 50–70% in 1-year post-ablation compared to 10–30%

Address correspondence to Ravi Ranjan, Department of Biomedical Engineering, University of Utah, Salt Lake City, UT, USA. Electronic mail: ravi.ranjan@hsc.utah.edu

Published online: 05 August 2022

while using antiarrhythmic drugs.[13,33] Isolation of pulmonary veins is the cornerstone of ablation therapy for paroxysmal AF patients.[4] As AF progresses and becomes persistent, AF mechanisms become more complicated, and pulmonary vein isolation alone is not as effective long-term[3]; and as a result, operators often target additional areas like the posterior wall or fractionated electrograms to improve the outcomes; However, none of the current methods have shown consistently better outcomes for persistent AF.[10,11,17,21,28]

In persistent AF patients, electrical and structural remodeling play important roles in the initiation and maintenance of AF. The excess amounts of fibrotic areas, which are anchoring points for drivers and rotors, contribute to the maintenance of AF waves in persistent AF patients.[12] As we have shown in our recent study, the size of the contiguous areas available for fibrillatory waves to propagate (we are calling fibrillatory areas (FA)) is an important determinant for the maintenance of arrhythmia.[14] Based on the critical mass hypothesis, if there is not enough available tissue for depolarization to keep fibrillatory waves sustained, as a consequence of tissue being in the refractory period, the activation will not be self-sustaining, and the arrhythmia will stop. This concept is well supported by reported outcomes in patients undergoing surgical maze procedures.[8,27,34]

In this study, we used patient-specific geometries with incorporated fibrosis and scar patterns in a group of persistent AF patients who underwent AF ablation to validate the concept that smaller FAs result in better outcomes, which correlates with the clinical observation. After showing the high accuracy of the computational models in matching the clinical ablation outcomes, we further suggested additional ablation lines that limit FAs to stop AF in a patient-specific manner through a tailored ablation simulation approach for patients with arrythmia recurrence. We also simulated the effects of three common antiarrhythmic drugs to test if they can terminate the rotor activity in patients with recurrence post-ablation and compared the simulation result with clinical outcome. Such patient-specific modeling can potentially lead to reducing the need for repeat ablations and the associated time and cost through precision ablation aimed to reduce available FAs.

METHODS

Patient Selection

Persistent AF patients (n = 30) were selected for this study who underwent initial AF RF ablation at the University of Utah. Left atrial RF ablation was done as previously described[36] with each patient undergoing pulmonary vein isolation with some patients undergoing additional ablation lines targeting mostly the posterior wall based upon operator discretion. The ablation was done using radiofrequency ablation after getting two transeptal left atrial access under intracardiac echocardiography (ICE) and fluoroscopy guidance. An activated clotting time (ACT) of 350 to 400 was maintained giving heparin as needed during the procedure. The pulmonary vein isolation was checked with the Lasso catheter. For RF a range of power, force and duration was used with 30 W lesions lasting 10 to 30 s and 50 W lesions lasting 5 to 10 s. These patients had a 3-month post-ablation late gadolinium enhancement (LGE)-MRI and at least two years of subsequent AF recurrence follow-up data. The recurrence data post-90-day blanking was obtained based on chart review from ECG and Holter or monitored cardiac telemetry data as well as clinic notes from follow up visits to the cardiologist or electrophysiologist or the emergency room. The selected 30 patients were a subgroup (the first alphabetically ordered in the lists) of the patient population from our previous study, with 15 patients from each group of with and without arrhythmia recurrence.[14] This retrospective study was approved by the Institutional Review Board at the University of Utah.

MRI Acquisition

LGE-MRI scans were done on clinical scanners (Siemens Healthcare, Erlangen, Germany) 15 min after injection of contrast agent (0.1 mmol/kg, Multihance, Bracco Diagnostic Inc., Princeton, NJ) using an institutional standard inversion recovery prepared, 3-D gradient echo pulse sequence as described.[22] The LGE-MRI scans were acquired with a voxel size of 1.25 mm × 1.25 mm × 2.5 mm and reconstructed to voxel spacing of 0.625 mm × 0.625 mm × 1.25 mm.

3D Patient-Specific Atrial Geometric Models

We used a median image filter with a radius of 1 pixel on the LGE-MRIs to reduce the effect of noise. Segmentation of the left atrial wall was performed manually for each slice as described before.[19] Fibrosis and ablation scar were detected on the segmented left atrial wall of pre and post-ablation LGE-MRIs, respectively, using Corview image processing software (University of Utah, Utah, USA) and automatic thresholding with K-means clustering method.[23] The signal to noise ratio of the post-ablation scar is much

higher and hence the use of pre-ablation MRI to detect fibrosis and the post-ablation MRI to detect ablation scar. The mesh generation process is explained in detail in our previous paper.[14] Briefly, it involved exporting the wall segmentation of the post-ablation scan from Corview to MATLAB (Release 2016a, The MathWorks, Inc., Natick, Massachusetts, United States) to create a smooth tetrahedral mesh. We registered the before ablation geometry with fibrosis pattern to the after-ablation geometry with ablation scar pattern using iterative closest point (ICP) along with affine registration methods to get a final atrial geometry with added ablation scar on top of fibrosis. The final mesh was refined, and modified using FreeCAD (Juergen Riegel *et al*., Version 0.17 Available from http://www.freecadweb.org) and MeshLab (Cignoni, Paolo, *et al*., Version 2016.12. Available from http://www.meshlab.net). The total number of mesh elements ranged from 800,000 to 1,000,000 based on the size of the atrium, with an average length of about 400 μm. Fiber orientation was estimated for our patient-specific models by registering our geometries to an atlas heart model with known fiber orientations.[18]

Electrophysiological Model Parameterization

We used Courtemanche cellular model for modeling atrial action potential[6] and modified the membrane parameters to reproduce realistic human action potential curves as measured by Kim *et al.* during chronic AF.[16] The Ito (transient outward K+), ICaL (L-type Ca2+), and IK1 (inward rectifier K+) currents were reduced to 80%, 20%, and 90% of their normal value, respectively, and IKr (rapid component of the delayed rectifier K+ current) was increased by 60%.[24] Fibrotic regions, as well as scarred regions, were simulated by incorporating reduced inward rectifier potassium current (50%), L-type calcium current (30%), and sodium current (80%). Monodomain formulation was used for simulating the electrical propagation with the longitudinal conductivity of 0.1064 mS/mm and transverse and normal conductivity of 0.0152 mS/mm for normal myocyte (Conduction velocity of 1.2 m/s along the fiber orientation and 0.6 m/s in other directions). Fibrosis was modeled with the longitudinal conductivity of 0.0546 mS/mm, and transverse and normal conductivity of 0.0068 mS/mm as previously used by Zahid *et al.*[38] (Conduction velocity of 0.6 m/s along the fiber orientation and 0.05 m/s in other directions). The conductivities and conduction velocities of the scar in different directions were reduced by a factor of 10 when compared to fibrotic tissue.

Simulation of Electrical Activity

We used CARPentry software package[31] within the python-based carputils framework[32] for creating computational AF models to further investigate the importance of the size of FAs and gaps in ablation lines in the ability of the model to sustain AF. The simulations were run on 16 or 8 core processors. The computation time required for running 10 s simulations from each pacing location ranged from ~ 7 to ~ 11 h across the patients based on the size of the LA.

Protocol for Checking the AF Inducibility of the Models

For each model, we chose five different pacing sites based on anatomical landmarks (between the left pulmonary veins, the lower part of the atrium on the mitral isthmus line closer to the mitral valve, the tip of the appendage, mid anterior wall, and between right pulmonary veins). We chose a strength of 200 μA/cm^2 of 10 ms duration and paced the models with two beat pacing train with a cycle length of 400 ms followed by a third extra stimulus with a decreasing coupling interval going down from 340 to 200 ms in 20 ms decrements. Simulations were run for 10 s from the last pacing stimulus. We considered AF to be self-sustaining in a model if there was sustained rotor activity until the end of the simulation (10 s).

Simulating the Effects of Antiarrhythmic Drugs

Conventional antiarrhythmic drugs are classified based on their main mechanisms of action.[35] We selected three commonly used antiarrhythmic drugs and simulated the percentages of blocking of different ion channels at different concentrations of these drugs based on the reported values in Table 1.[9] We simulated a class 1c drug, Flecainide, and Class III drugs, Sotalol and Amiodarone. We ran the simulations with ion channel block against all tested ion currents at free plasma C_{max} (maximum or peak concentration at the recommended dose in the drug label) values of $1 \times C_{max}$ and $3 \times C_{max}$ for the patients with unsuccessful ablation.

Calculation of Fibrillatory Areas and Creation of Additional Ablation Lines to Minimize the Fibrillatory Areas

After detecting ablation scar on the LA geometry based on post-ablation MRI, we divided the atrium into five regions based on LA landmarks and the pattern of scar around the pulmonary vein ostium after wide antral ablation attempts for all the ablations. Region 1 was the area around the left sided pulmonary

TABLE 1. The percentages of blocking of different ion channels at different concentrations of the selected antiarrhythmic drugs.

Antiarrhythmic drug	Cav1.2	hERG	Kv4.3	Nav1.5-late	Nav1.5-peak
Amiodarone					
Block (%) at free C_{max} = 0.7 nM	1.3	1.6	4.1	3.5	0.2
Block (%) at 3 × free C_{max}	2.4	2.9	6	5.1	0.3
Sotalol					
Block (%) at free C_{max} = 146,986.4 nM		15.9			
Block (%) at 3 × free C_{max}		34.7			
Flecainide					
Block (%) at free C_{max} = 752.9 nM	0.8	51.8	13.8	11	1.6
Block (%) at 3 × free C_{max}	3.4	73	26.3	20.1	11.4

veins, region 2 was the area surrounding the right sided pulmonary veins, region 3 was below the pulmonary veins in the lower part of the posterior wall, region 4 covered the anterior wall and region 5 was the appendage. This arrangement of region selection was based on large contiguous areas separated by standard ablation lines done as part of every clinical ablation for atrial fibrillation which involves ablating around the pulmonary veins. The borders of the regions were drawn in a way that they included the maximum scar that separated two adjacent regions as shown in Fig. 1. FAs were calculated as described in detail in our recently published work.[14] Briefly, it is a measure of contiguous surface area that is available for fibrillatory waves to propagate; the gaps in ablation lines between adjacent regions are accounted for by including a weighted sum of adjacent areas separated by ablation lines. The proportion of adjacent areas included in the calculation of the FA is dependent on the relative gap in the ablation line on the boundary between adjacent areas, with a larger gap leading to a larger FA as calculated by:

$$\mathrm{EA}_i = A_i - \textit{area of scar in } A_i,\ (i = 1:\ \text{region number}, 1:5) \tag{1}$$

where Effective Area $(\mathrm{EA})_i$ is the scar free area in region i; A_i is the surface area of region i; and for regions 1 to 5, FA_i was calculated as:

$$\mathrm{FA}_i = \mathrm{EA}_i + \sum_{j=1}^{\#\ of\ A_i\ neighbors} \frac{\Sigma\ lengths\ of\ the\ gaps\ on\ the\ shared\ border\ of\ A_i\ and\ A_j}{length\ of\ the\ shared\ border\ of\ A_i\ and\ A_j} \mathrm{EA}_j \tag{2}$$

A simplified schematic showing the quantification of FAs is shown in Fig. 2. In this Figure, the ablation scar is shown in red. There are three distinct regions A1, A2 and A3 separated by ablation lines with gaps in them. The EAs can be calculated by deducting the area of scar in each region from the surface area of that region as shown on the right image.

For e.g. A_2 is the total green area including scar (shown in red) in the left panel in Fig. 2, the green area in the right panel of Fig. 2 is EA_2 which does not include the scar in A_2.

For the waves that originate in A_1 ($i = 1$), FA_1 was calculated as:

$$\mathrm{FA}_1 = \mathrm{EA}_1 + \frac{x}{a}\mathrm{EA}_2 \tag{3}$$

where EA_1 is the effective area of region1, a is the total length of the shared border of A_1 and A_2, x is the length of the gap on that shared border, similarly for FA_2 and FA_3 we have:

$$\mathrm{FA}_2 = \mathrm{EA}_2 + \frac{x}{a}\mathrm{EA}_1 + \frac{y+z}{b}\mathrm{EA}_3 \tag{4}$$

$$\mathrm{FA}_3 = \mathrm{EA}_3 + \frac{y+z}{b}\mathrm{EA}_2 \tag{5}$$

where EA_2 is the effective area of region 2, b is the total length of the shared border between A_2 and A_3, y and z are the length of the gaps on the shared border between A_2 and A_3. FA_1 does not include contributions from A_3 as in this schematic, A_1 and A_3 have no shared boundary. Similarly, for FA_3 there is no contribution from A_1 as there is no shared boundary between A_1 and A_3.

After the calculation of FAs in patients that had recurrence after the initial ablation, we simulated the effect of an additional suggested ablation line by adding scar between the two largest calculated FAs by either filling the gaps in ablation lines or creating new lines on their shared border. The model was then run to check for the AF inducibility. If the model still showed sustained rotor activity, we added another line between the largest and the third-largest FA as well and ran the simulation again. This was done with the goal of minimizing the size of FAs.

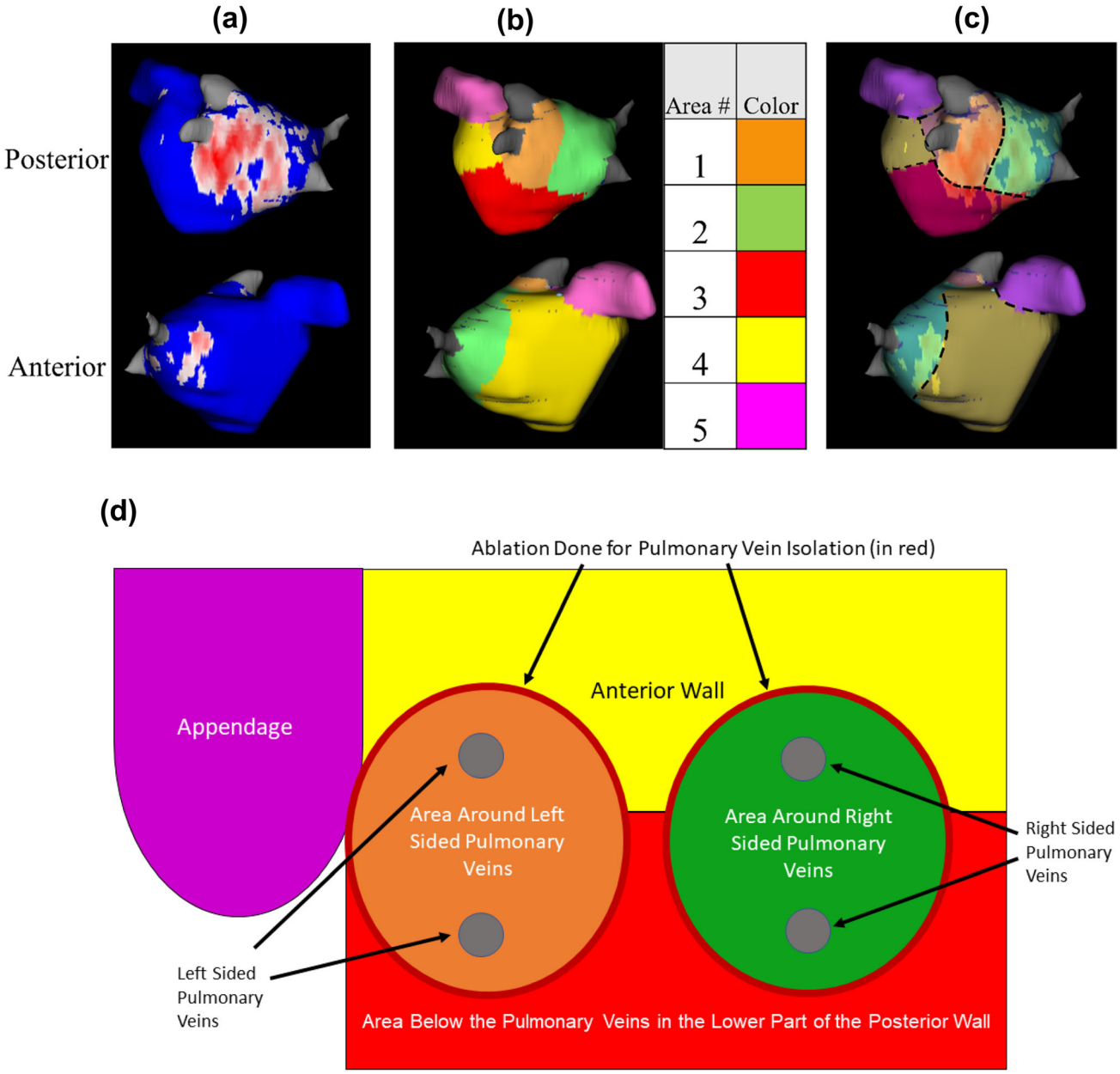

FIGURE 1. Region assignment for calculating FAs in an example patient. (a) This panel shows the segmented and processed post-ablation MRI with scar region shown in red and normal tissue in blue. Row one is the posterior view and row two is the anterior view. (b) The different regions marked with different colors along with their assigned numbers on the right side of the panel. (c) The assigned boundary lines (with dashed lines) between the different areas overlaid on the scar distribution. (d) A simplified schematic showing the logic behind region selections. The ovals around the pulmonary veins represents the wide antral catheter ablation line that is created around the pulmonary veins for all these patients.

Statistics and Analysis

Continuous variables were expressed as mean ± SD. P values < 0.05 indicate statistically significant results.

RESULTS

The selected patients for this study were a subgroup (first 15 alphabetically ordered in each group with or without recurrence post AF ablation) of the selected

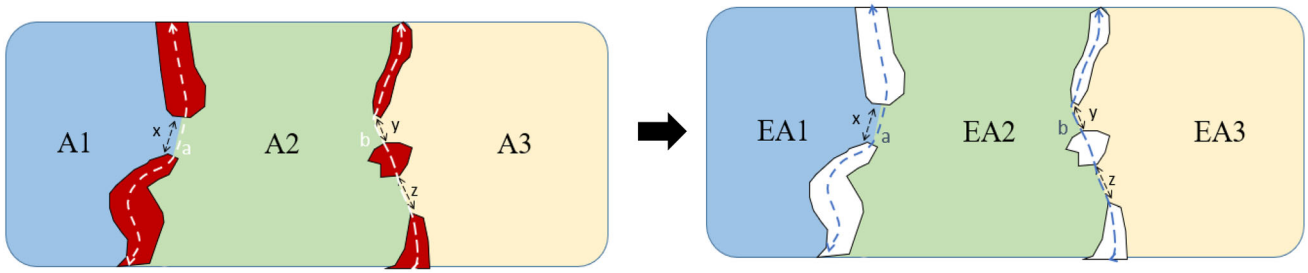

FIGURE 2. Simplified schematic showing the quantification of FAs. The ablation scar is shown in red. There are three distinct regions A1, A2 and A3 separated by ablation lines with gaps in them on the left image. The EAs were calculated by deducting the scarred region for each region from the surface area of that region as shown on the right image

patients in our previous study showing the importance of FAs in the recurrence of arrhythmia after ablation in persistent AF patients.[14] These two groups of the patients had similar total atrial wall area: (11,133 vs. 12,949 mm^2, $p < 0.21$) for patients with recurrence vs. patients with no recurrence post-ablation. The baseline patient demographics are shown in supplementary material Table 1 along with the type of medications that they were taking post ablation.

Checking the AF Inducibility of the Models

The average calculated FAs for patients with recurrence post-ablation (PersR) and patients with no recurrence (PersNR) after the first ablation are shown in Fig. 3. FA values along with the simulation result for each patient are reported in Supplementary Materials, Table 2. The average FA_{max} was significantly larger in the patients within the recurrence group compared to the no recurrence group (8517 ± 1444 vs. 6772 ± 1531 mm^2, $p < 0.001$). The simulations showed sustained rotor activity in 13 out of 15 models of patients with clinical recurrence (sensitivity, 86.7%, 95%CI 59.5 to 98.3) and showed no sustained rotor activity in 12 out of 15 models of patients with no clinical recurrence (specificity, 80.0%, 95%CI 51.9 to 95.7). Figure 4 shows an example of a simulation for a patient with no recurrence post-ablation, and Fig. 5 is an example of a patient with recurrence post-ablation. The simulation videos for these patients are submitted in the supplementary materials.

Simulating the Effects of Antiarrhythmic Drugs

The patients with successful ablation were off anti-arrhythmic drugs after ablation; Only one of those patients stayed on anti-arrhythmic drugs (amiodarone-sotalol) to avoid ventricular tachycardia. We simulated the effects of different concentrations of the antiarrhythmic drugs for the 15 patients with recurrence post-ablation. The summary of simulation outcomes and their correlation with clinical outcomes are shown in Fig. 6. Rotor activity was seen in 10 out of 15 (66.6%) PersR patients with both concentrations of Amiodarone. Both concentrations of Sotalol stopped the rotor activity in four more patients compared to when no Sotalol was used, with persistent rotor activity identified in 9 out of 15 (60%) of patients. The lower concentration of Flecainide showed persistent rotor activities in 9 out of 15 (60%) models, and simulations with higher Flecainide concentration showed persistent rotor activity in 7 out of 15 (46.7%). In 6 out of 15 patients with arrhythmia recurrence antiarrhythmic drugs were being used. For 3 patients that were on Flecainide post unsuccessful ablation, the simulations correctly suggested the termination of rotor activity in 2 of those patients and not being helpful in stopping the arrhythmia for the third patient. After unsuccessful ablation with recurrence, three patients were on Amiodarone. Simulations correctly suggested the termination of arrhythmia in one of the patients and the drug not helping in another patient. However, for the last patient, the simulation suggested that Amiodarone is not helpful while taking it helped the patient clinically.

The simulations of the effects of antiarrhythmic drugs correlated with the clinical outcome in 5 out of 6 patients, making the model 83.33% accurate.

Suggesting Patient-Specific Ablation Lines Based on Fibrillatory Areas

The locations of the suggested additional ablation lines to reduce FA sizes leading to no rotor activity in the simulations along with the final calculated FAs after adding the new lines are reported in Supplementary Materials, Table 3. The average value of FAs after adding the suggested ablation lines was compared to FAs in patients without recurrence post-ablation, and there was no significant difference as shown in Fig. 7. Figure 8 shows the simulation result for the patient shown in Fig. 5 after adding the suggested

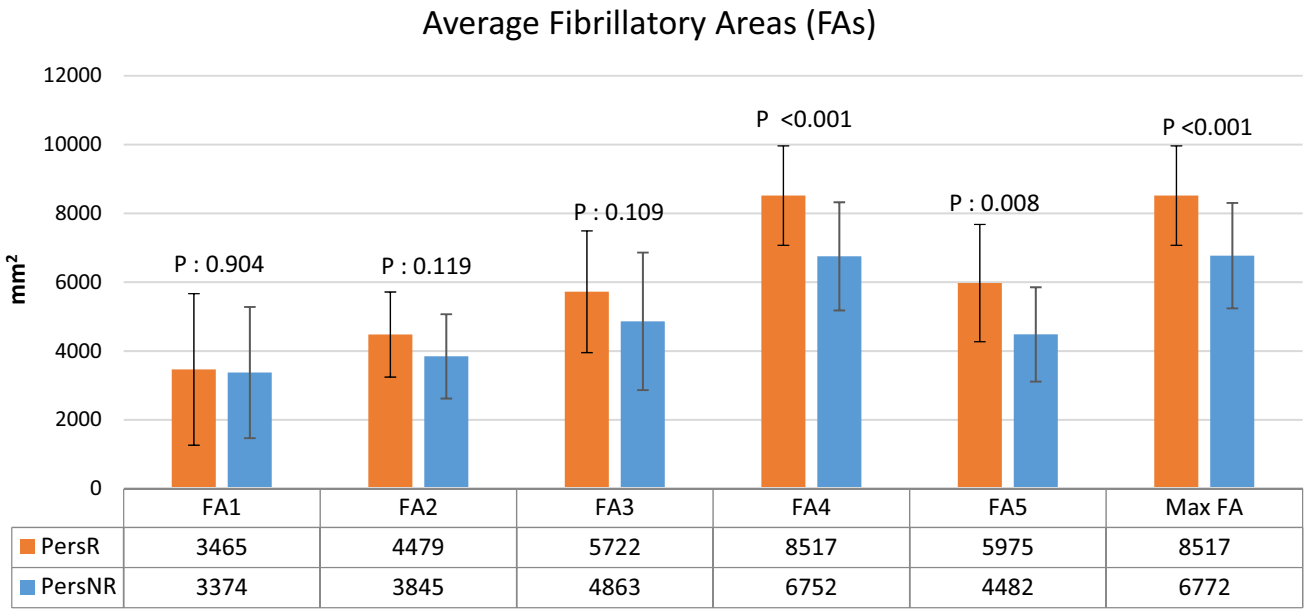

	FA1	FA2	FA3	FA4	FA5	Max FA
PersR	3465	4479	5722	8517	5975	8517
PersNR	3374	3845	4863	6752	4482	6772

FIGURE 3. Average fibrillatory areas (FA) in mm^2 for patients with recurrence post ablation (PersR, *n* = 15) vs. patients without recurrence post ablation (PersNR, *n* = 15).

ablation lines leading to no sustained rotor activity. The simulation video for this patient before and after adding the additional line is submitted in the Supplementary Materials. The suggested additional lines were between the appendage and anterior wall (region 4) as well as between the bottom part of the LA and the anterior wall on the left side (close to the left pulmonary veins). It is important to notice that as shown in this Figure, for this patient and the other patients, when we needed to add a line between region 4 and 5, the appendage (region 5) was not fully isolated and either shared a gap on its border with region 1 (left pulmonary veins) or we did not completely isolate region 4 and 5 and left a small gap for the signal to reach the appendage from region 4. This approach is intentional in order to prevent complete appendage isolation leading to thromboembolic risks.[26,29]

DISCUSSION

The objective of this study was to create reliable computational patient-specific AF models that can predict the outcome of ablation and be used for suggesting additional ablation lines that can prevent AF recurrence. We also showed the high accuracy of our computational models in predicting the effect of antiarrhythmic drugs. We explored the importance of the size of the contiguous two-dimensional area that is available for fibrillatory waves to sustain themselves and then used that concept to suggest the additional ablation lines for stopping AF recurrence in patient-specific models. Our patient-specific computational models predict clinical outcomes after ablation with an accuracy of 83.33% (25 out of 30 patients). The models confirm the significance of FAs in sustaining AF,[14] and allow us to test the value of inserting additional ablation lines with the goal of minimizing the FAs. In our models with the added ablation lines for patients with arrhythmia recurrence post initial ablation, the FA was smaller and led to no recurrence of AF. Our computational models also showed high accuracy for anticipating the effect of antiarrhythmic drugs (83.33%) (5 out of 6 patients). However, the number of patients was limited, and there is a need to further investigate the accuracy of the models for simulating the effects of antiarrhythmic drugs with a larger number of patients.

The concept of using additional ablation lines after pulmonary vein isolation has been tested before in STAR AF II trial, and it did not result in significant improvement in clinical outcomes.[30] It is plausible that the routine use of additional lines might not be an effective strategy across a broad range of atrial sizes with variant baseline fibrosis and scar, but patient-specific models taking into consideration the existing fibrosis, scar and anatomic nuances may be quite effective. The fibrotic areas as well as scarred regions act as anchoring points for drivers and rotors and contribute to the maintenance of AF waves in persistent AF patients.[12] Good quality atrial MRI can reliably quantify atrial geometry and detect post-ablation scar as shown by us and others.[5,15] That additional information can be used within a therapeutic strategy when planning redo procedures in these patients. Moreover, complicating our understanding of STAR

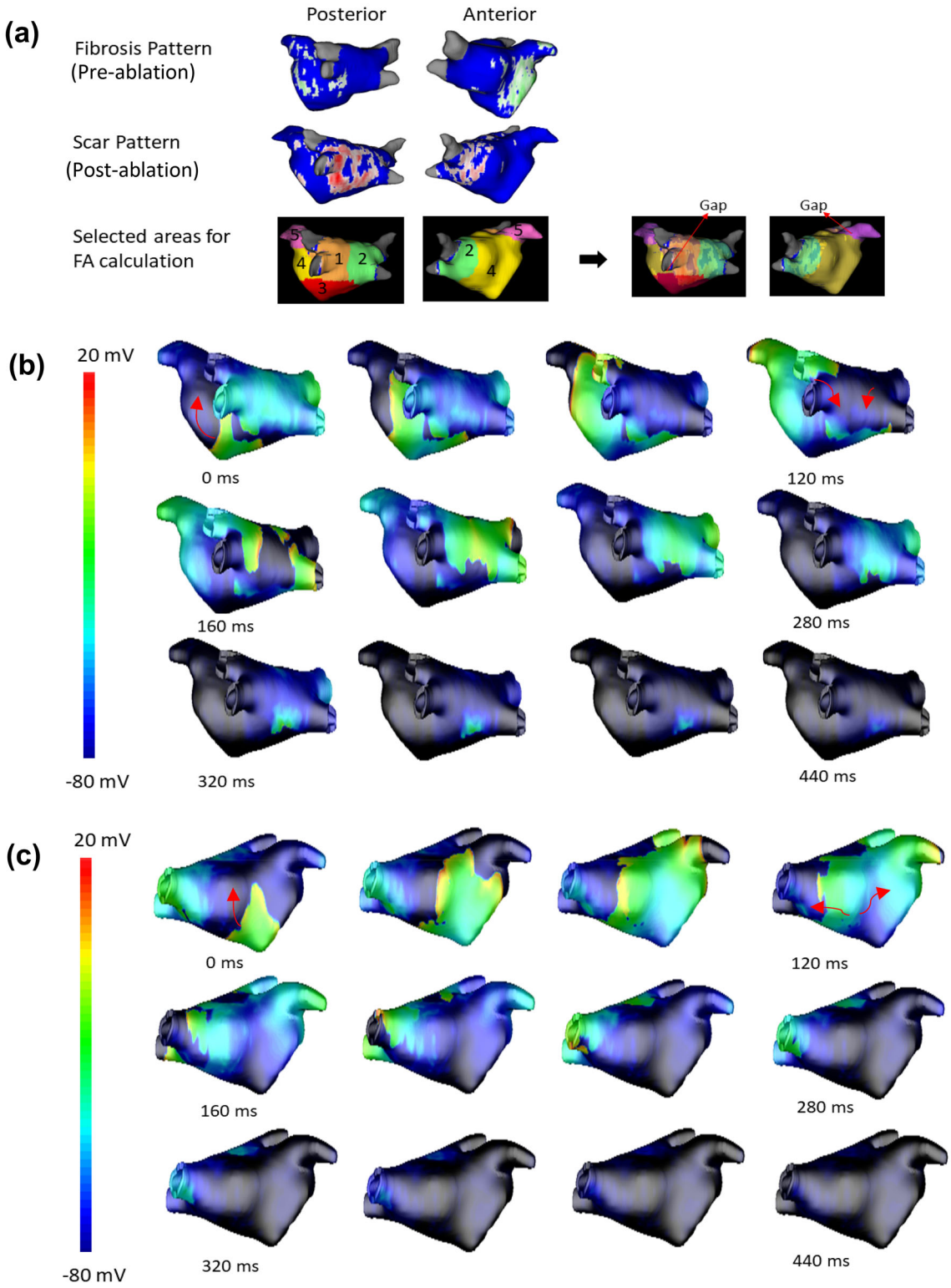

FIGURE 4. 3D LA simulation results from a patient showing rotor activity that terminates before the end of simulation (10 s) in a patient with no-arrhythmia recurrence post-ablation. (a) Fibrosis (in green) and scar (in red) in the left atrium based on pre-ablation and post-ablation MRI, respectively, used in the model along with the different regions used for FA calculation are shown. Gaps in the scar through which activation spreads to adjacent regions is marked on the right had panels. Snap shots of the transmembrane potential in the LA wall at different time points are shown in panels (b) Posterior view and (c) Anterior view.

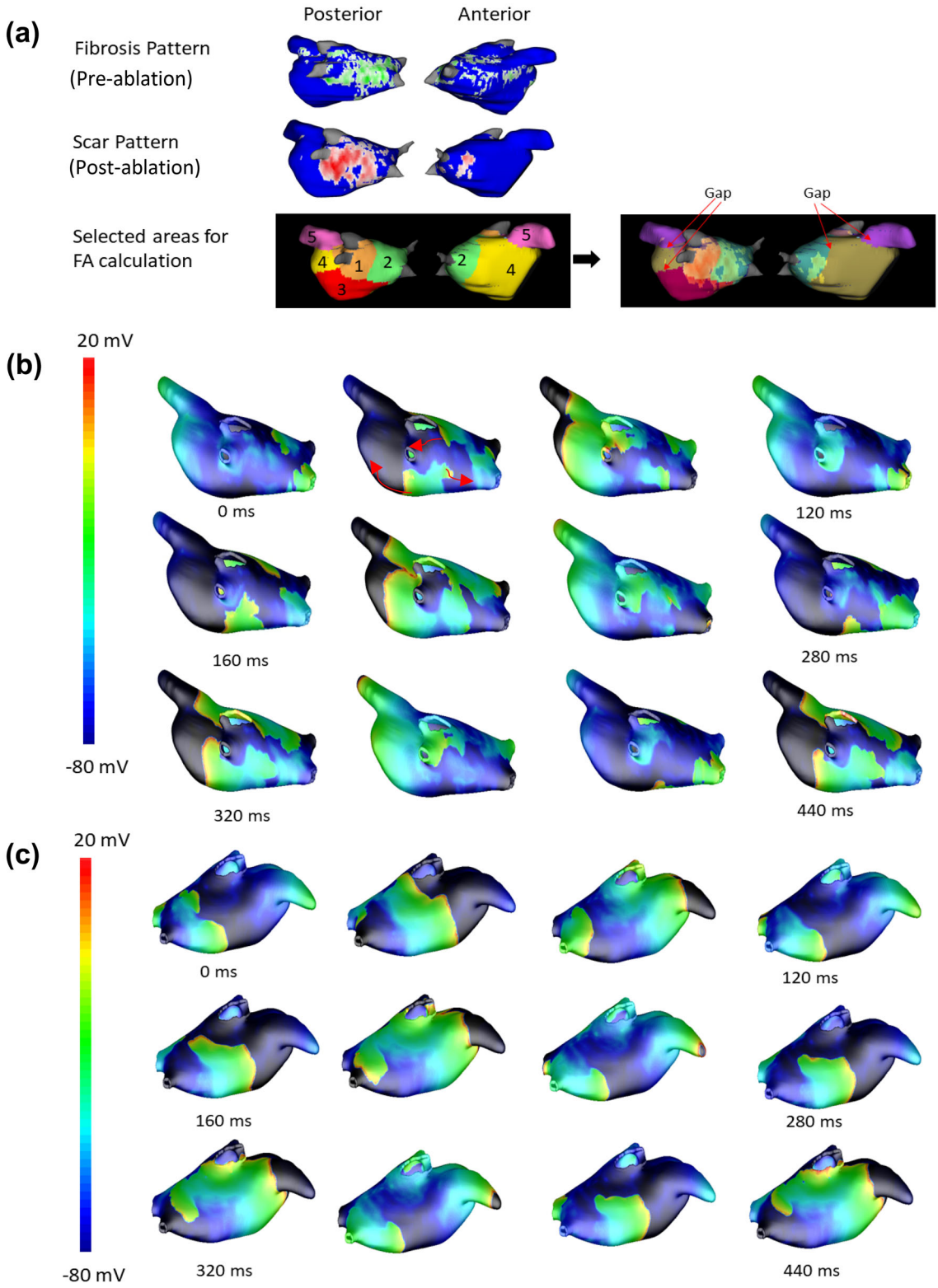

FIGURE 5. 3D LA simulation results from a patient showing rotor activity that sustained until the end of simulation (10 s) in a patient with arrhythmia recurrence post-ablation. (a) Fibrosis (in green) and scar (in red) in the left atrium based on pre-ablation MRI and post-ablation MRI, respectively, used in the model along with the different regions used for FA calculation are shown. Gaps in the scar through which activation spreads to adjacent regions is marked on the right had panels. Snap shots of the transmembrane potential in the LA wall at different time points are shown in panels (b) Posterior view and (c) Anterior view.

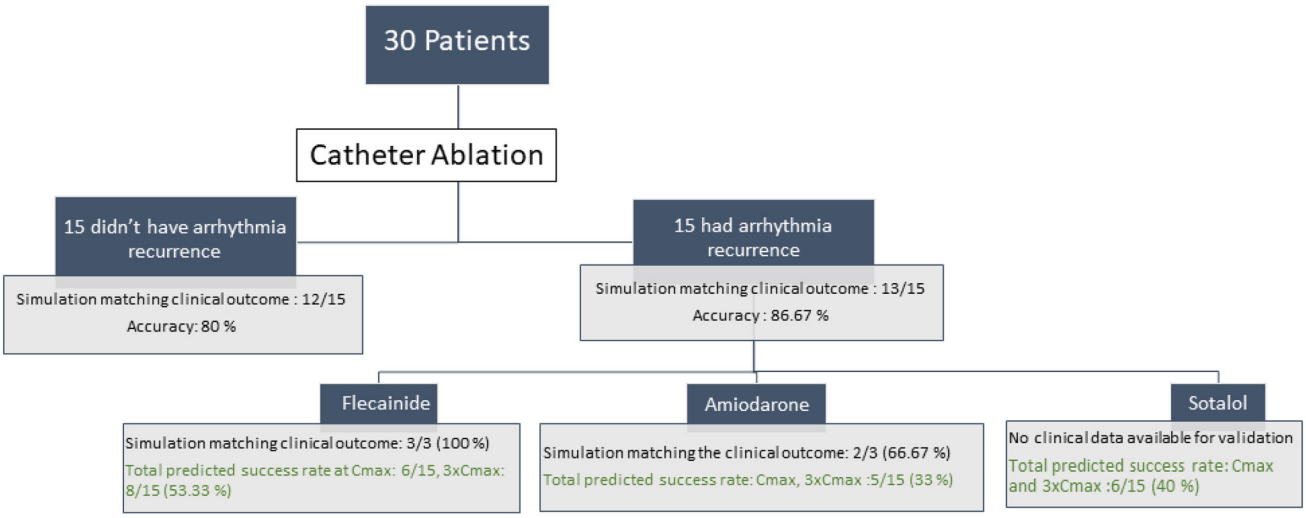

FIGURE 6. Summary of simulation outcomes and their correlation with clinical outcomes. Six patients with recurrence post ablation were on anti-arrhythmics. Simulation was done with all three anti-arrhythmics for all 15 patients that had recurrence. Results of simulation with anti-arrhythmics is shown for all those patients and separately compared for the six patients that were clinically on anti-arrhythmics.

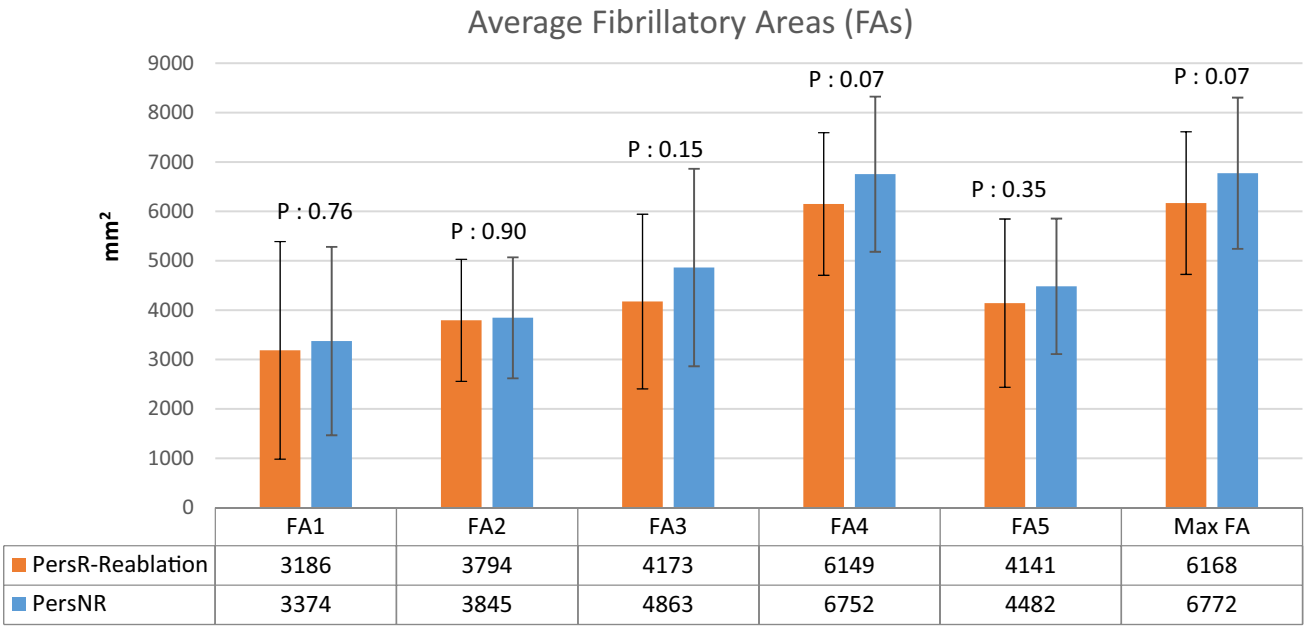

	FA1	FA2	FA3	FA4	FA5	Max FA
PersR-Reablation	3186	3794	4173	6149	4141	6168
PersNR	3374	3845	4863	6752	4482	6772

FIGURE 7. Average fibrillatory areas (FA) in mm^2 for patients with recurrence post ablation after the suggested re-ablation (PersR-Reablation, *n* = 15) vs. patients without recurrence post ablation (PersNR, *n* = 15).

AF II results is that it was done in the pre-contact force era, and for ablation lines to be effective, they must be complete. Numerous groups, including us, have shown that in that era, as much as 50% of the targeted area did not result in permanent scar.[22,36]

The strongest evidence suggesting the importance of limiting the area available for fibrillatory waves to propagate and sustain itself comes from AF recurrence data after the surgical Cox-Maze procedure. The cut and sew Cox-Maze procedure was based upon the AF genesis theory of multiple-circuit reentry, with inherent complete lines, founded upon the concept of introducing lesions to abolish areas critical to maintaining reentry.[7] The long-term success rates after Cox-Maze procedures are more than 80% off antiarrhythmic drugs, which is much better than outcomes after catheter ablation.[34]

Recently OPTIMA simulation ablation method has been introduced which has shown promising results.[2] However, the addition of proposed lines in our simu-

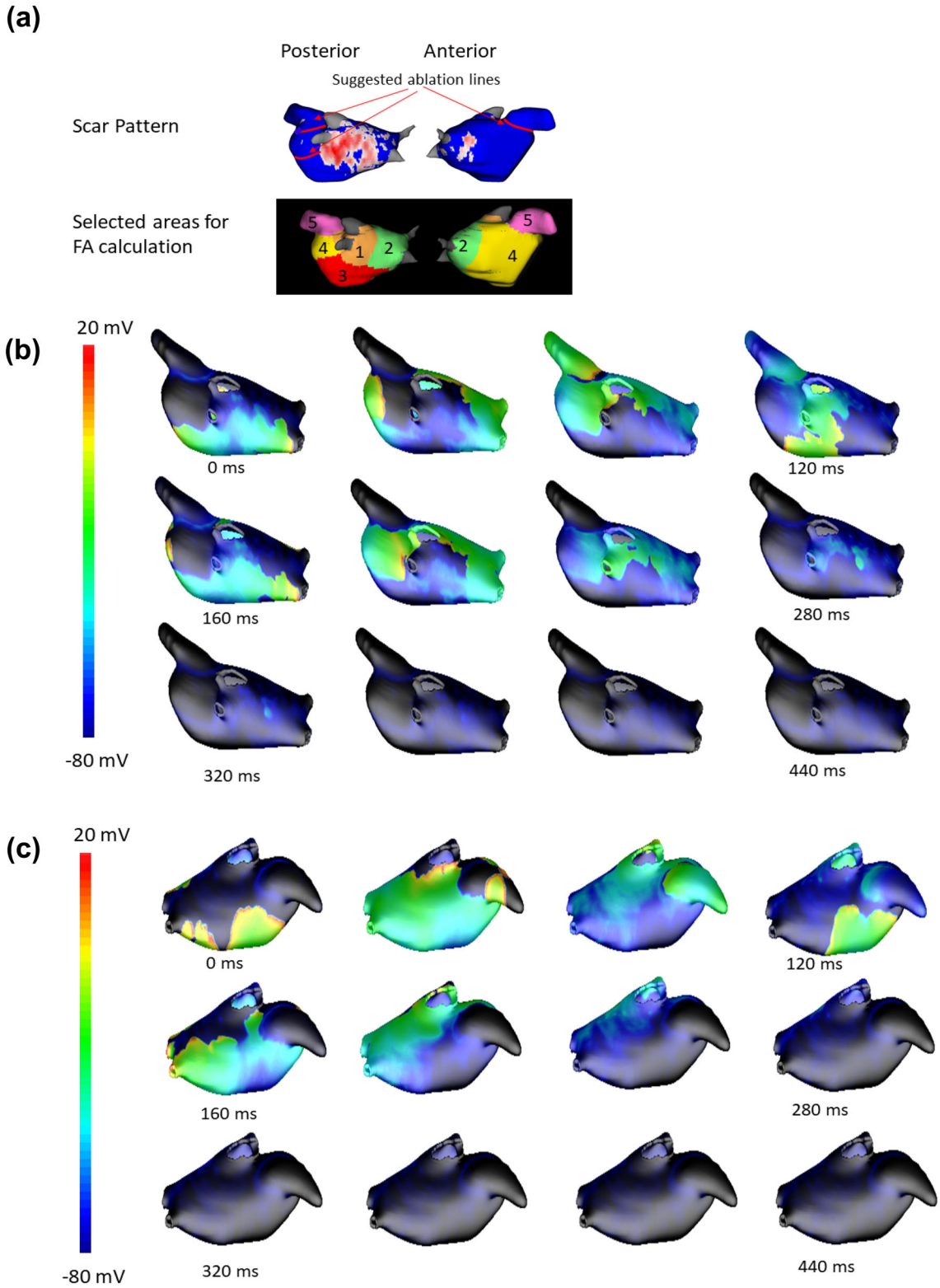

FIGURE 8. 3D LA simulation results from a patient that had recurrence and simulation showed sustained activity now with additional ablation lines that results in termination of the arrhythmia. (a) Scar based on post-ablation MRI along with suggested ablation line shown in red line between the different regions to lower the FA. Snap shots of the transmembrane potential in the LA wall at different time points are shown in panels (b) Posterior view and (c) Anterior view showing the lack of sustained activity.

lation was based on anatomical sites where most of the ablation is done in clinic, including wide antral ablation for pulmonary vein isolation. This makes it quite plausible to test this concept further in a clinical study without significant changes to the current practice of ablation, where the pulmonary vein isolation forms the cornerstone of catheter ablation strategies. The geographical FA regions have been chosen by keeping the current ablation patterns in mind. As shown in Fig. 8, the additional line added is only on the anterior base of the appendage so that it does not isolate it completely and create complications of thrombus within the appendage requiring a closure device and appendage ligation. And yet, despite not isolating the appendage completely, we clearly reduce the FA size and, as such, predict an improvement in ablation outcomes. Other clinical studies have shown improvement with isolating the appendage, which might be consistent with reduced FA.[25,37]

Persistent AF continues to have only moderate levels of ablation related success despite trying numerous approaches beyond pulmonary vein isolation. Numerous approaches ranging from targeting drivers, continuous fractionated areas to posterior wall debulking have been tried but none of them have significantly improved the outcomes. This is likely due to the inherently more complex pathophysiology of the problem. We suspect that as the disease progresses from paroxysmal to persistent the disease becomes more complex and might not be driven by only focal areas and might be also related to re-entrant activities; hence just targeting them might not be sufficient. The wavelet theory and the critical mass hypothesis have long been used to explain such persistent atrial fibrillation once it is beyond being driven by fixed drivers. The approach tested here uses those fundamental concepts and creates an individualized plan based on patient specific anatomies. Our technique also adapts for the inevitable gaps in ablation lines that are present when doing the procedure percutaneously. We have incorporated the contribution of adjoining areas in a weighted manner when calculating the Fibrillatory Area. The validation of the fundamental aspect comes from the surgical technique where the results have been quite encouraging. The use of personalized computational models allows us to further develop a patient specific strategy for ablation for patients with persistent AF.

In conclusion, patient-specific ablation models can be used for predicting arrhythmia outcomes post-ablation in patients with persistent AF. These computational models can also be used to test outcomes after creating new ablation lines that limit the area available for fibrillatory waves to sustain itself and may allow patient-specific tailored ablation approaches to improve long-term outcomes in patients with persistent AF. The models might also be useful in predicting the effects of antiarrhythmics for these patients.

Limitations

We showed the high accuracy of our models in predicting the effect of certain ablation patterns /antiarrhythmics by comparing the simulation with clinical outcome. However, the accuracy of our models with the suggested additional ablation lines for patients with recurrence need to be tested in a prospective clinical study. The number of patients for checking the accuracy of the models in predicting the effects of antiarrhythmics were also limited and another study is needed to thoroughly investigate that. We included patient-specific geometry along with fibrosis and post-ablation scar patterns and estimated fiber orientation. The estimation of fiber orientation might decrease the accuracy of the models. The right atrium was excluded from our simulation because right atrium is not part of clinical ablation for atrial fibrillation in the vast majority of cases where ablation is focused on the left atrium. There are also report that the right atrium has minimal contribution to persistent AF.[20] Adding the right atrium it might result in a more accurate model. We did not include patient specific electrophysiological parameters as it was not available for these patients and potentially can further improve simulation predictions.

FUNDING

RR is or reently has been a consultant to Abbott, Biosense Webster and Medtronic. The University of Utah has research grants from Biosense Webster and Abbott with RR as the PI. JB has research grants from Boehringer Ingelheim, Boston Scientific, Altathera. The remaining authors have nothing to disclose. RR is currently supported by NHLBI R01 HL142913.

SUPPLEMENTARY INFORMATION

The online version contains supplementary material available at https://doi.org/10.1007/s10439-022-03029-5.

CONFLICT OF INTEREST No benefits in any form have been or will be received from a commercial party related directly or indirectly to the subject of this manuscript.

REFERENCES

[1]Andrade, J., P. Khairy, D. Dobrev, and S. Nattel. The clinical profile and pathophysiology of atrial fibrillation: relationships among clinical features, epidemiology, and mechanisms. *Circ. Res.* 114:1453–1468, 2014.

[2]Boyle, P. M., T. Zghaib, S. Zahid, R. L. Ali, D. Deng, W. H. Franceschi, J. B. Hakim, M. J. Murphy, A. Prakosa, and S. L. Zimmerman. Computationally guided personalized targeted ablation of persistent atrial fibrillation. *Nat. Biomed. Eng*. 3:870–879, 2019.

[3]Calkins, H., J. Brugada, D. L. Packer, R. Cappato, S.-A. Chen, H. J. Crijns, R. J. Damiano Jr., D. W. Davies, D. E. Haines, and M. Haissaguerre. Hrs/ehra/ecas Expert Consensus Statement on Catheter and Surgical Ablation of Atrial Fibrillation: Recommendations for Personnel, Policy, Procedures and Follow-up: A report of the Heart Rhythm Society (hrs) Task Force on Catheter and Surgical Ablation of Atrial Fibrillation developed in partnership with the European Heart Rhythm Association (ehra) and the European Cardiac Arrhythmia Society (ecas); in collaboration with the American College of Cardiology (acc), American Heart Association (aha), and the Society of Thoracic Surgeons (sts). Endorsed and Approved by the governing bodies of the American College of Cardiology, the American Heart Association, the European Cardiac Arrhythmia Society, the European Heart Rhythm Association, the Society of Thoracic Surgeons, and the Heart Rhythm Society. *Europace*. 9:335–379, 2007.

[4]Calkins, H., K. H. Kuck, R. Cappato, J. Brugada, A. J. Camm, S.-A. Chen, H. J. Crijns, R. J. Damiano Jr., D. W. Davies, and J. DiMarco. HRS/EHRA/ECAS expert consensus statement on catheter and surgical ablation of atrial fibrillation: recommendations for patient selection, procedural techniques, patient management and follow-up, definitions, endpoints, and research trial design: a report of the Heart Rhythm Society (HRS) Task Force on Catheter and Surgical Ablation of Atrial Fibrillation. Developed in partnership with the European Heart Rhythm Association (EHRA), a registered branch of the European Society of Cardiology (ESC) and the European Cardiac Arrhythmia Society (ECAS); and in collaboration with the American College of Cardiology (ACC), American Heart Association (AHA), the Asia Pacific Heart Rhythm Society (APHRS), and the Society of Thoracic Surgeons (STS). Endorsed by the governing bodies of the American College of Cardiology Foundation, the American Heart Association, the European Cardiac Arrhythmia Society, the European Heart Rhythm Association, the Society of Thoracic Surgeons, the Asia Pacific Heart Rhythm Society, and the Heart Rhythm Society. *Europace*. 14:528–606, 2012.

[5]Chubb, H., R. Karim, S. Roujol, M. Nuñez-Garcia, S. E. Williams, J. Whitaker, J. Harrison, C. Butakoff, O. Camara, and A. Chiribiri. The reproducibility of late gadolinium enhancement cardiovascular magnetic resonance imaging of post-ablation atrial scar: a cross-over study. *J. Cardiovasc. Magn. Reson*. 20:21, 2018.

[6]Courtemanche, M., R. J. Ramirez, and S. Nattel. Ionic mechanisms underlying human atrial action potential properties: insights from a mathematical model. *Am. J. Physiol.-Heart Circ. Physiol*. 275:H301–H321, 1998.

[7]Cox, J. L. Atrial fibrillation II: rationale for surgical treatment. *J. Thorac. Cardiovasc. Surg*. 126:1693–1699, 2003.

[8]Cox J. L., R. B. Schuessler and J. P. Boineau. The development of the Maze procedure for the treatment of atrial fibrillation. In: Seminars in Thoracic and Cardiovascular Surgery. Elsevier, 2000, pp. 2–14.

[9]Crumb, W. J., Jr., J. Vicente, L. Johannesen, and D. G. Strauss. An evaluation of 30 clinical drugs against the comprehensive in vitro proarrhythmia assay (CiPA) proposed ion channel panel. *J. Pharmacol. Toxicol. Methods*. 81:251–262, 2016.

[10]Fink, T., M. Schlüter, C.-H. Heeger, C. Lemes, T. Maurer, B. Reissmann, J. Riedl, L. Rottner, F. Santoro, and B. Schmidt. Stand-alone pulmonary vein isolation versus pulmonary vein isolation with additional substrate modification as index ablation procedures in patients with persistent and long-standing persistent atrial fibrillation: the randomized Alster-Lost-AF Trial (Ablation at St. Georg Hospital for Long-Standing Persistent Atrial Fibrillation). *Circulation*. 10:e005114, 2017.

[11]Haissaguerre, M., M. Hocini, A. Denis, A. J. Shah, Y. Komatsu, S. Yamashita, M. Daly, S. Amraoui, S. Zellerhoff, and M.-Q. Picat. Driver domains in persistent atrial fibrillation. *Circulation*. 130:530–538, 2014.

[12]Haissaguerre, M., A. J. Shah, H. Cochet, M. Hocini, R. Dubois, I. Efimov, E. Vigmond, O. Bernus, and N. Trayanova. Intermittent drivers anchoring to structural heterogeneities as a major pathophysiological mechanism of human persistent atrial fibrillation. *J. Physiol*. 594:2387–2398, 2016.

[13]Jaïs, P., B. Cauchemez, L. Macle, E. Daoud, P. Khairy, R. Subbiah, M. Hocini, F. Extramiana, F. Sacher, and P. Bordachar. Catheter ablation versus antiarrhythmic drugs for atrial fibrillation: the A4 study. *Circulation*. 118:2498–2505, 2008.

[14]Kamali, R., J. Kump, E. Ghafoori, M. Lange, N. Hu, T. J. Bunch, D. J. Dosdall, R. S. Macleod, and R. Ranjan. Area available for atrial fibrillation to propagate is an important determinant of recurrence after ablation. *JACC Clin. Electrophysiol*. 7:896–908, 2021.

[15]Kamali, R., J. Schroeder, E. DiBella, B. Steinberg, F. Han, D. J. Dosdall, R. S. Macleod, and R. Ranjan. Reproducibility of clinical late gadolinium enhancement magnetic resonance imaging in detecting left atrial scar after atrial fibrillation ablation. *J. Cardiovasc. Electrophysiol*. 31:2824–2832, 2020.

[16]Kim, B.-S., Y.-H. Kim, G.-S. Hwang, H.-N. Pak, S. C. Lee, W. J. Shim, D. J. Oh, and Y. M. Ro. Action potential duration restitution kinetics in human atrial fibrillation. *J. Am. Coll. Cardiol*. 39:1329–1336, 2002.

[17]Knecht, S., M. Hocini, M. Wright, N. Lellouche, M. D. O'Neill, S. Matsuo, I. Nault, V. S. Chauhan, K. J. Makati, and M. Bevilacqua. Left atrial linear lesions are required for successful treatment of persistent atrial fibrillation. *Eur. Heart J*. 29:2359–2366, 2008.

[18]Krueger M. W., V. Schmidt, C. Tobón, F. M. Weber, C. Lorenz, D. U. Keller, H. Barschdorf, M. Burdumy, P. Neher and G. Plank. Modeling atrial fiber orientation in patient-specific geometries: a semi-automatic rule-based approach. In: *International Conference on Functional Imaging and Modeling of the Heart*. Springer, 2011, pp. 223–232.

[19]McGann, C., N. Akoum, A. Patel, E. Kholmovski, P. Revelo, K. Damal, B. Wilson, J. Cates, A. Harrison, and R. Ranjan. Atrial fibrillation ablation outcome is predicted by left atrial remodeling on MRI. *Circulation*. 113:000689, 2013.

[20]Oral, H., A. Chugh, E. Good, T. Crawford, J. F. Sarrazin, M. Kuhne, N. Chalfoun, D. Wells, W. Boonyapisit, and N. Gadeela. Randomized evaluation of right atrial ablation after left atrial ablation of complex fractionated atrial electrograms for long-lasting persistent atrial fibrillation. *Circulation*. 1:6–13, 2008.

[21]Ouyang, F., S. Ernst, J. Chun, D. Bänsch, Y. Li, A. Schaumann, H. Mavrakis, X. Liu, F. T. Deger, and B. Schmidt. Electrophysiological findings during ablation of persistent atrial fibrillation with electroanatomic mapping and double Lasso catheter technique. *Circulation*. 112:3038–3048, 2005.

[22]Parmar, B. R., T. R. Jarrett, N. S. Burgon, E. G. Kholmovski, N. W. Akoum, N. Hu, R. S. Macleod, N. F. Marrouche, and R. Ranjan. Comparison of left atrial area marked ablated in electroanatomical maps with scar in MRI. *J. Cardiovasc. Electrophysiol*. 25:457–463, 2014.

[23]Perry D., A. Morris, N. Burgon, C. McGann, R. MacLeod and J. Cates. Automatic classification of scar tissue in late gadolinium enhancement cardiac MRI for the assessment of left-atrial wall injury after radiofrequency ablation. In: *Medical Imaging 2012: Computer-Aided Diagnosis*International Society for Optics and Photonics, 2012, p. 83151D.

[24]Ramos-Mondragón, R., C. A. Galindo, and G. Avila. Role of TGF-β on cardiac structural and electrical remodeling. *Vasc. Health Risk Manag*. 4:1289, 2008.

[25]Romero, J., L. Di Biase, S. Mohanty, C. Trivedi, K. Patel, M. Parides, I. Alviz, J. C. Diaz, V. Natale, and J. Sanchez. Long-term outcomes of left atrial appendage electrical isolation in patients with nonparoxysmal atrial fibrillation: a propensity score-matched analysis. *Circulation*. 13:e008390, 2020.

[26]Safavi-Naeini, P., and A. Rasekh. Left atrial appendage closure and pulmonary vein isolation. *Texas Heart Inst. J*. 47:60–62, 2020.

[27]Schaff H. V., J. A. Dearani, R. G. Daly, T. A. Orszulak and G. K. Danielson. Cox-Maze procedure for atrial fibrillation: Mayo Clinic experience. In: *Seminars in Thoracic and Cardiovascular Surgery*. Elsevier, 2000, p. 30–37.

[28]Scherr, D., P. Khairy, S. Miyazaki, V. Aurillac-Lavignolle, P. Pascale, S. B. Wilton, K. Ramoul, Y. Komatsu, L. Roten, and A. Jadidi. Five-year outcome of catheter ablation of persistent atrial fibrillation using termination of atrial fibrillation as a procedural endpoint. *Circulation*. 8:18–24, 2015.

[29]Tilz R. R., B. Schmidt, S. D. Menon, K. Chun, A. Fuernkranz, A. Metzner, B. Koektuerk, M. Konstantinidou, T. Zerm and R. Malesius. Left atrial appendage function and clinical outcome after electrical isolation of left atrial appendage in patients undergoing atrial fibrillation ablation. Am. Heart Assoc., 2008.

[30]Verma, A., C.-Y. Jiang, T. R. Betts, J. Chen, I. Deisenhofer, R. Mantovan, L. Macle, C. A. Morillo, W. Haverkamp, and R. Weerasooriya. Approaches to catheter ablation for persistent atrial fibrillation. *N. Engl. J. Med*. 372:1812–1822, 2015.

[31]Vigmond, E., R. W. dos Santos, A. J. Prassl, M. Deo, G. Plank, and S. Bauer. Solvers for the cardiac bidomain equations. *Prog. Biophys. Mol. Biol*. 96:3–18, 2007.

[32]Vigmond, E. J., M. Hughes, G. Plank, and L. J. Leon. Computational tools for modeling electrical activity in cardiac tissue. *J. Electrocardiol*. 36:69–74, 2003.

[33]Wazni, O. M., N. F. Marrouche, D. O. Martin, A. Verma, M. Bhargava, W. Saliba, D. Bash, R. Schweikert, J. Brachmann, and J. Gunther. Radiofrequency ablation vs antiarrhythmic drugs as first-line treatment of symptomatic atrial fibrillation: a randomized trial. *Jama*. 293:2634–2640, 2005.

[34]Weimar, T., S. Schena, M. S. Bailey, H. S. Maniar, R. B. Schuessler, J. L. Cox, and R. J. Damiano Jr. The cox-maze procedure for lone atrial fibrillation: a single-center experience over 2 decades. *Circulation*. 5:8–14, 2012.

[35]Williams, E. V. Classification of antidysrhythmic drugs. *Pharmacol. Therap*. 1:115–138, 1975.

[36]Yamashita, K., R. Kamali, E. Kwan, R. S. MacLeod, D. J. Dosdall, and R. Ranjan. Effective ablation settings that predict chronic scar after left atrial ablation. *JACC*. 6:143–152, 2020.

[37]Yorgun, H., U. Canpolat, M. Okşul, Y. Z. Şener, A. H. Ateş, H. J. Crijns, and K. Aytemir. Long-term outcomes of cryoballoon-based left atrial appendage isolation in addition to pulmonary vein isolation in persistent atrial fibrillation. *EP Europace*. 21:1653–1662, 2019.

[38]Zahid, S., H. Cochet, P. M. Boyle, E. L. Schwarz, K. N. Whyte, E. J. Vigmond, R. Dubois, M. Hocini, M. Haïssaguerre, and P. Jaïs. Patient-derived models link re-entrant driver localization in atrial fibrillation to fibrosis spatial pattern. *Cardiovasc. Res*. 110:443–454, 2016.